Journal of Neuroimmunology 333 (2019) 476962

Contents lists available at ScienceDirect

Journal of Neuroimmunology

journal homepage: www.elsevier.com/locate/jneuroim

Propofol reduces microglia activation and neurotoxicity through inhibition of extracellular vesicle release

Jianhui Liu[a,c], Yuju Li[b,c], Xiaohuan Xia[b], Xiaoyu Yang[a], Runze Zhao[c], Justin Peer[c], Hongyun Wang[c], Zenghan Tong[c], Fengtong Gao[c], Hai Lin[c], Beiqing Wu[c], Yunlong Huang[b,c,*], Jialin C. Zheng[b,c,*]

[a] Department of Anesthesiology, Tongji Hospital affiliated to Tongji University School of Medicine, Shanghai, China
[b] Center for Translational Neurodegeneration and Regenerative Therapy, Shanghai Tenth People's Hospital affiliated to Tongji University School of Medicine, Shanghai, China
[c] Department of Pharmacology and Experimental Neuroscience, University of Nebraska Medical Center, Omaha, NE 68198, United States

ARTICLE INFO

Keywords:
Anesthetics
Extracellular vesicles
Neuroinflammation
Microglia
Neurotoxicity
Propofol

ABSTRACT

Propofol is an established anesthetic widely used for induction and maintenance of anesthesia. We investigated propofol for its anti-inflammatory effects on microglia and found that propofol treatment is associated with substantial lower levels of extracellular vesicles (EVs) in immune activated microglia. Importantly, EVs collected from immune activated microglia reversed propofol-mediated anti-inflammatory and neuroprotective effects, suggesting that propofol reduces proinflammatory microglia activation and microglia-mediated neurotoxicity through inhibition of EV release. These data shed new insight into a novel molecular mechanism of propofol-mediated neuroprotective and immunomodulatory effects through inhibition of EV release.

1. Introduction

In neurological diseases, such as Alzheimer's disease, Parkinson's disease, multiple sclerosis, and epilepsy, chronic neuroinflammation has been observed and often postulated as a central component in the disease progression (Amor and Woodroofe, 2014; McGeer and McGeer, 2013). Microglial cells, the brain-resident macrophage cell type, constantly survey the brain parenchyma to maintain homeostasis. During neuroinflammation, microglia change into active phenotypes to enhance phagocytosis and secrete a plethora of factors critical for central nervous system (CNS) repair and regeneration. However, aberrant and prolonged activation of microglia can lead to brain degeneration and neuronal death rather than neuroprotection (Gonzalez-Scarano and Baltuch, 1999). Interestingly, microglia are an active cell type that secretes abundant levels of extracellular vesicles (EVs), which are membrane-enclosed vesicles that include exosomes and microvesicles (Fruhbeis et al., 2013; Joshi et al., 2014; Stevens et al., 2007). EVs can be found in interstitial fluid, cerebrospinal fluid (Vella et al., 2008), circulating blood (Suetsugu et al., 2013), and primarily assert biological function through delivering cytokines, nucleic acids, lipids, and proteins to nearby or distant cells, suggesting that they play an important role in cell-to-cell communication (Thery et al., 2006). EV secretion is increased during neuroinflammation; our previous studies, along with others', have suggested that EVs fuel pathogenic processes in the brain during neuroinflammation (Gupta and Pulliam, 2014; Huang et al., 2018; Wang et al., 2017; Wu et al., 2015; Wu et al., 2018).

Propofol is a short-acting intravenous anesthetic agent that is widely used in surgeries. It is often the choice of medication for the starting and maintenance of general anesthesia or for the sedation of mechanically ventilated adults and patients undergoing diagnostic or invasive procedures (Kochhar et al., 2016). Like most anesthetics, propofol is believed to work at least partly via the γ-aminobutyric acid (GABA) receptor (Trapani et al., 2000). Other mechanisms of action by propofol may include cannabinoid receptors (Fowler, 2004). Increasing evidence from *in vitro* and *in vivo* studies indicates that propofol is able to modulate microglial activation and may assert anti-inflammatory effects (Gui et al., 2012; Huang et al., 2009; Liu et al., 2012; Wang et al., 2010). However, the mechanism underlying propofol-induced anti-inflammatory action remains to be fully elucidated.

In the present study, we investigated a novel EV-mediated

* Corresponding author at: Center for Translational Neurodegeneration and Regenerative Therapy, Shanghai Tenth People's Hospital affiliated to Tongji University School of Medicine, Shanghai 200072, China; Department of Pharmacology and Experimental Neuroscience, University of Nebraska Medical Center, Omaha, NE 68198, United States.
E-mail addresses: yhuan1@unmc.edu (Y. Huang), jialinzheng@tongji.edu.cn (J.C. Zheng).

https://doi.org/10.1016/j.jneuroim.2019.05.003
Reçu le 27 décembre 2018; Reçu en forme révisée le 28 mars 2019; accepté le 3 mai 2019

mechanism that accounts for propofol-induced anti-inflammatory and neuroprotective effects in immune-activated microglial cells. We hypothesized that propofol exhibits its anti-inflammatory and neuroprotective effects through the down-regulation of immune-activated EV release. We found that the anti-inflammatory and neuroprotective effects of propofol can be reversed by the addition of EVs collected from immune activated microglia, suggesting that propofol reduces microglia activation and neurotoxicity through inhibition of EV release. Therefore, these studies support a new mechanism of propofol for the neuroprotective and immunomodulatory effects in the CNS.

2. Methods

2.1. Cell culture and reagents

BV2 microglial cells were purchased from the American Type Culture Collection (ATCC, Rockville, MD). The neuroblastoma cell line Neuro2a (N2A) was obtained from the ATCC by Dr. Zeljka Korade as described and provided to us (Korade et al., 2009). Both cell lines were cultured in Dulbecco's modified Eagle's medium (Gibco, Gaithersburg, MD, USA) supplemented with 10% fetal bovine serum, 100 U/mL penicillin, and 100 μg/mL streptomycin in a humidified 95% air - 5% CO_2 incubator at 37 °C. Propofol and lipopolysaccharide (LPS) were purchased from Sigma (St Louis, MO, USA). Propofol was dissolved in 0.1% methanol and protected from light throughout each experiment. For all propofol treatment groups, equal concentrations of methanol were used as vehicle controls.

2.2. Immunocytochemistry

The cultured cells were fixed in 4% paraformaldehyde for 20 min at room temperature and then incubated with methanol for 20 min at −20 °C. Fixed cells were blocked with 3% bovine serum albumin in PBS and then incubated with primary antibodies to CD11b (BD Biosciences, San Diego, CA), TuJ1 (Class III β-tubulin, Sigma), or MAP2 (Millipore, Billerica, MA, and Bio-Rad, Hercules, CA) overnight. At the second day, the cells were washed with PBS three times and incubated for 1 h at room temperature with the secondary anti-mouse IgG antibody (coupled with green dye, Alexa Flour 488, Molecular Probes, Eugene, Oregon). Nuclear DNA were labeled with 4′, 6-diamidino-2-phenylindole (DAPI; Sigma-Aldrich, St. Louis, MO) for 10 min after the secondary antibody at room temperature. Cover slips were mounted on glass slides with mounting medium (Sigma-Aldrich). For TUNEL assay, N2A cells were fixed and permeabilized with 0.5% Triton-X, and the apoptotic cells were determined by in situ cell death detection kit with Fluorescein (Roche, Basel, Switzerland, www.roche-applied-science.com) according to the manufacture's protocol. Fluorescent images were obtained using a Zeiss 710 Confocal Laser Scanning Microscope (Carl Zeiss, Oberkochen, Germany). All images were imported into Image-ProPlus, version 7.0 (Media Cybernetics, Inc., Rockville, MD, www.mediacy.com) for quantifying number of apoptotic cells. The assessors were blinded during image acquisition or quantification.

2.3. Cell viability

BV2 microglia cells were seeded in 12-well plates and grown overnight and then treated with 10, 30, or 100 μM propofol for 24 h in the absence or presence of 10 ng/mL LPS. To determine the effect of propofol on cell viability, a colorimetric CellTiter 96® AQueous One Solution Assay, also known as the MTS (3-(4,5-dimethylthiazol-2-yl)-5-(3-carboxymethoxyphenyl)-2-(4-sulfophenyl)-2H-tetrazolium) assay, was performed based on the manufacture's instruction (Promega, Madison, WI) as previously described (Huang et al., 2018). Briefly, assays were performed by adding 10% (*v*/v) MTS and an electron coupling reagent (phenazine ethosulfate; PES) directly to culture wells, incubating for 1 h, and then recording absorbance at 490 nm with a 96-well microplate reader (Multiskan sk3; Thermo Lab Systems, Beverly, MA, USA).

2.4. Isolation of EVs

EVs were isolated from the serum-free culture medium of BV2 cells by a differential centrifugation protocol described previously using the same BV2 cells (Suetsugu et al., 2013; Wu et al., 2015; Wu et al., 2018). Briefly, the supernatants were first centrifuged at 500 ×*g* for 5 min to remove the free cells, followed by 2000 ×*g* for 20 min to remove cellular debris, and then at 10,000 ×*g* for 30 min to remove intracellular organelles. Lastly, EVs were collected by ultracentrifugation at 100,000 ×*g* for 70 min at 4 °C.

2.5. Nanoparticle tracking analysis (NTA)

The size and number of EVs were assessed with a NanoSight NS300 system (Malvern Instruments, Malvern, UK). BV2 cells were cultured in 12-well culture plates for 1 day before treatment with propofol. At 24 h after treatment with propofol, EVs were isolated from normalized volumes of serum-free culture supernatants through differential centrifugation and resuspended with 60 μL phosphate buffered saline (PBS). The supernatant was diluted to 1:100 in PBS, and 1 mL of solution was used for NTA, which was performed at room temperature. Furthermore, the temperature was measured for each analysis and manually entered into the system. The software used for capturing and analyzing the data was NTA 2.2 Build 0381. Each sample was measured 5 × 60 s, and for each of these measurements a new portion of the sample was injected. The result for each sample was presented as an average of the 5 measurements.

2.6. Real-time polymerase chain reaction (PCR) assays

Total RNA from the BV2 cells was isolated with TRIzol Reagent (Thermo Fisher Scientific, Waltham, MA) and RNeasy Kit (Qiagen Inc., Hilden, Germany) according to the manufacturer's protocol. Primers used for real-time RT-PCR included interleukin (IL)-1 (Assay ID Mm00434228), Tumor Necrosis Factor alpha (TNF-α) (Assay ID Mm00443258), Nitricoxidesynthase2 (NOS2) (Assay ID Mm00440502), IL-10 (Assay ID Mm01288386), and GAPDH (Assay ID Mm99999915), which were purchased from Thermo Fisher Scientific. Real-time RT-PCR was performed using the 1-step quantitative TaqMan assay in a StepOne Real-Time PCR system (Applied Biosystems). Relative IL-1, TNF, NOS2, and IL-10 mRNA levels were determined and standardized with a GAPDH internal control using a comparative ΔΔCT method. All primers used in the study were tested for amplification efficiencies and the results were similar.

2.7. Western blot

Protein concentrations were determined by a Bradford protein assay. Sodium dodecyl sulfate polyacrylamide gel electrophoresis was performed to separate proteins from whole-cell and EV lysates, using M-PER mammalian protein extraction reagent (Thermo Fisher Scientific). After electrophoretic transfer to polyvinyl difluoridene membranes (Millipore), the membranes were incubated overnight at 4 °C with polyclonal antibodies for tissue transglutaminase (tTG, Neomarkers, Fremont, CA, USA), and flotillin-2 (Cell Signaling Technology, Danvers, MA, USA), followed by horseradish peroxidase-linked secondary anti-rabbit (1:5000) or anti-mouse (1:10000) secondary antibodies (Cell Signaling Technology). Antigen-antibody complexes were visualized by Pierce ECL Western Blotting Substrate (Thermo Fisher Scientific). For quantification of the data, films were scanned with a CanonScan 9950 F scanner (Ota, Tokyo, Japan) and images were analyzed using the public domain NIH ImageJ program (http://rsb.info.nih.gov/nih-image/).

2.8. MAP2 ELISA

N2A cells were plated in 96-well plates at concentrations of 2×10^4 cells per well. MAP-2 neuronal antigen was determined using colorimetric ELISA as described previously. (Constantino et al., 2011; Huang et al., 2011) Briefly, N2A cells were blocked with 3% normal goat serum in phosphate buffered saline and incubated for 1 h with antibodies against MAP-2 (Millipore), followed by anti-mouse biotinylated antibody (VECTOR Laboratories) for 30 min. Avidin/biotin complex solution (VECTOR Laboratories) was added for 30 min, then color was developed using TMB substrate (Sigma-Aldrich) and terminated with 1 M H_2SO4 (Sigma-Aldrich). The absorbance was read at 450 nm using a microplate reader (Bio-Rad Laboratories, Hercules, CA). N2A culture wells in the same plate that had undergone the same procedure but were incubated without anti-MAP-2 primary antibody were used as negative control and for background subtraction.

2.9. Statistical analysis

Data were evaluated statistically by the analysis of variance, followed by Tukey's test for multiple comparisons. Data were shown as mean ± SD. The asterisk (*) and double asterisk (**) denote $p < .05$ and $p < .01$, respectively, compared with control. The pound sign (#) and double pound sign (##) denote $p < .05$, $p < .01$, respectively, compared with the LPS-treated groups.

3. Results

3.1. Propofol inhibits immune activation of microglia

To determine the effect of propofol on the innate immune activation in the brain, we used a BV2 cell line to model the microglia. The BV2 cells were characterized by CD11b expression, with > 95% of cells in the culture positive for CD11b (Supplementary Fig. 1). We treated BV2 microglial cells with 10, 30, or 100 μM propofol for 24 h either in the absence or presence of LPS. Propofol treatment at these doses did not significantly change BV2 cell viability (Supplementary Fig. 2A). Similarly, same doses of propofol treatment did not affect the viability of LPS-activated microglia (Supplementary Fig. 2B). Subsequent experiments were performed with propofol at the treatment concentration of 30 μM, which is consistent with the reported 95% effective concentration of propofol for loss of consciousness in the clinic (Smith et al., 1994). We determined the expression levels of inflammatory and anti-inflammatory genes after LPS and propofol treatment. LPS treatment induced significantly higher expression levels of classically activated (M1) microglial genes, which included IL-1β, TNF-α, and nitric oxide synthase 2 (NOS2) (Fig. 1A-C). In contrast, LPS treatment induced significantly lower expression levels of alternative activated (M2) microglial genes such as IL-10, CD206, and Ym1 (Fig. 1D-F). Therefore, propofol treatment induced opposite gene regulation compared to LPS.

To determine the effects of propofol on immune-activated microglia, we pre-treated microglia with propofol and then added LPS (10 ng/mL) for 24 h. Because microglia regularly patrol the CNS environment and are potent inducers of inflammation after LPS treatment, we used pretreatment to see the maximum benefit of proposal. Propofol pretreatment dose-dependently decreased the expressions of M1-specific marker genes including IL-1, TNF, NOS2, and increased M2-specific genes IL-10, CD206, and Ym1 in LPS-activated microglia (Fig. 1G-L). Together, these data suggest that propofol dampens the inflammatory phenotype of microglia after LPS activation.

3.2. Propofol inhibits activated microglia-mediated neurotoxicity

To determine whether the alteration of the microglia inflammatory phenotypes is associated with neuroprotective effects, we tested the neurotoxic potential of propofol-treated microglial cells using a previously established assay (Huang et al., 2011; Wu et al., 2015). N2A cell line was originally developed from a neuroblastoma. Upon differentiation, N2A cells predominantly expressed neuronal markers TuJ1, which is a marker for immature postmitotic neurons (Supplementary Fig. 3). Fewer number of N2A cells also expressed MAP2, which is a marker for mature neurons (Supplementary Fig. 3). We obtained supernatants from LPS-activated microglia with and without propofol pretreatment and used the cell-free supernatants as conditioned medium (microglia-conditioned medium) to treat the N2A neuronal cell line for neurotoxicity. As a positive control for the neurotoxicity assay, glutamate treatment significantly decreased neuronal viability (Fig. 2), consistent with previous reports (Choi et al., 1987; Finkbeiner and Stevens, 1988). Conditioned medium from LPS-stimulated microglia significantly reduced neuronal viability. Furthermore, pretreatment with propofol rescued the neurotoxicity by LPS-activated microglia conditioned medium (Fig. 2), indicating that activated microglia mediates neurotoxicity through soluble factors and propofol is able to abrogate this neurotoxic pathway.

3.3. Propofol reduces EV release from LPS-stimulated microglia

To determine the mechanism(s) of anti-inflammation by propofol, we investigated the roles of EV in this process. To quantify EV release, we isolated EVs from serum-free culture supernatants through differentiation centrifugation method as we previously described (Huang et al., 2018; Wu et al., 2015). We resuspended the EV pellets in PBS and characterized EV markers and sizes/concentrations through Western blotting and NTA tracking analysis, respectively. Western blotting determination revealed the presence of the EV markers flotillin-2 and tissue transglutaminase (tTG) in the protein lysates derived from the EV pellets (Fig. 3A). These two markers are known to be active components of EVs. (Antonyak et al., 2011; Oksvold et al., 2014) In addition to the EV markers, we have extensively tested levels of subcellular organelles, including markers PMP70 (for peroxisome), LAMP-1 (for lysosome), and VDAC (for mitochondria) and found that they were not detectable in our EV lysates in Western blots (Supplemental Fig. S4). To ensure that EVs were isolated from the same amount of cells, we also determined β-actin levels in whole cell lysates. β-actin levels were comparable among all treatment group. Quantification of flotillin-2 and tTG in EVs against β-actin in whole cell lysates identified that LPS dramatically increased the levels of flotillin-2 and tTG in the EV lysates, confirming that immune activation increases EV biogenesis in BV2 microglia (Fig. 3B, C). Furthermore, propofol treatment significantly decreased the protein levels of flotillin-2 (Fig. 3B) and tTG (Fig. 3C) in the EVs isolated from the LPS-stimulated microglial cells. Consistent with the Western blots, NTA tracking analysis revealed that LPS or propofol treatment did not change the sizes of EV but more specifically changed the concentrations of EVs (Fig. 3D-F). Quantification of EVs revealed that the concentration of EVs was upregulated by the LPS by nearly 65%, and propofol reversed the LPS-induced EV release from BV2 cells (Fig. 3D, F). The aforementioned experiments were performed using propofol pretreatment. To determine whether propofol has similar effects when it is used in treatment after LPS activation, we performed additional experiments and found that post-treatment with propofol also reduces flotllin-2 and tTG in EV lysates (Supplemental Fig. S5A–C), and decrease EV particle concentrations (Supplemental Fig. S5D–F), suggesting that treatment with propofol after LPS activation is able to reduce EV release from microglia.

3.4. Propofol inhibits LPS-stimulated inflammatory responses in microglia through reduction of EV release

To determine the roles of EV on propofol-mediated anti-inflammatory response in microglia, we investigated whether the anti-inflammation effects of propofol could be reversed by the addition of EVs isolated from immune-activated microglia. We collected EVs from

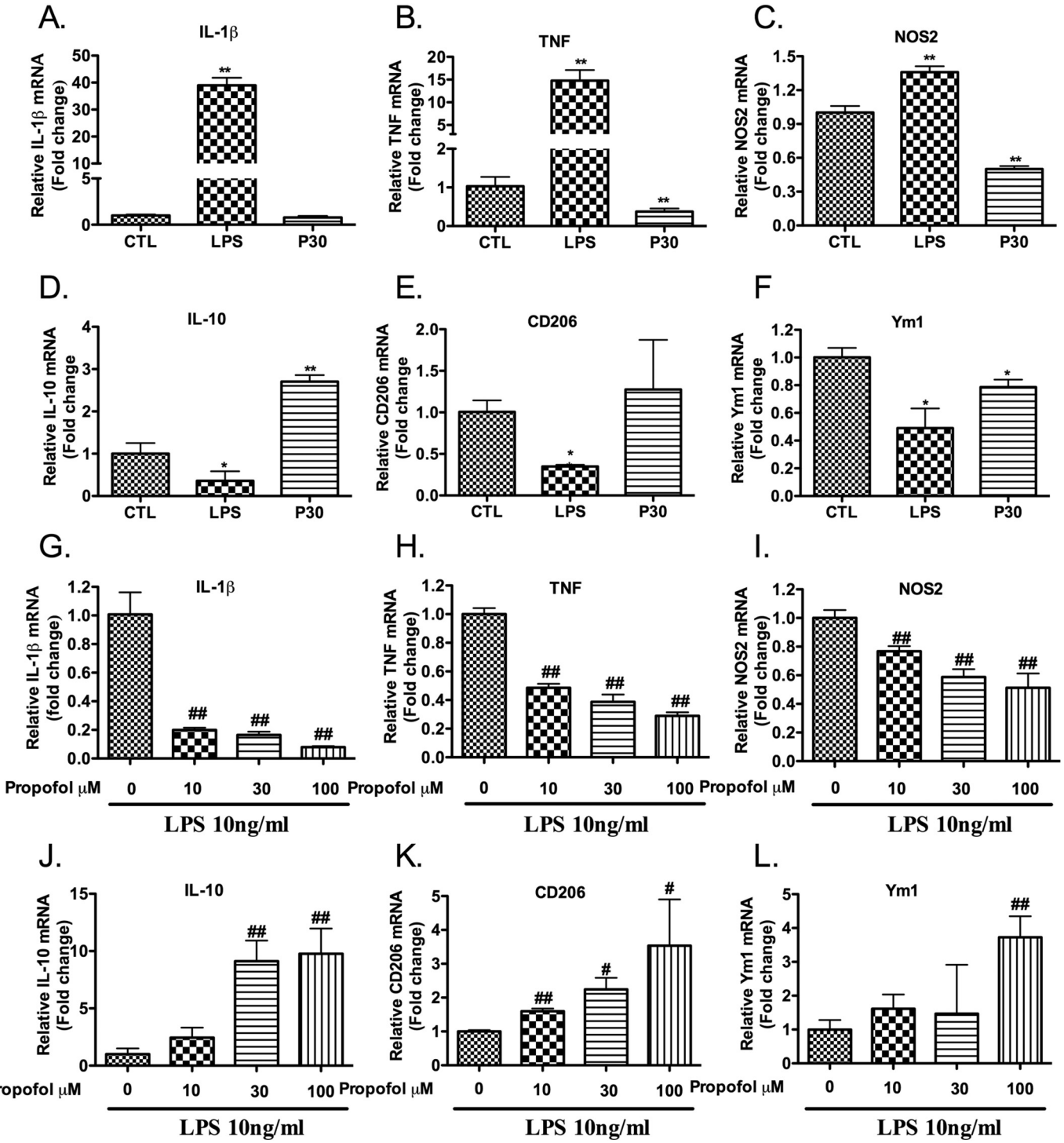

Fig. 1. Propofol blocks LPS-mediated gene expression alterations in activated microglia. (A-D) BV2 microglia cells were treated with LPS (10 ng/mL) or propofol (30 μM) for 24 h before total cellular RNA was isolated. Levels of IL-1β (A), TNF (B), NOS2 (C), IL-10 (D), CD206 (E), and Ym1 (F) gene expressions were determined through real time RT-PCR. (G-L) BV2 microglia cells were pre-treated with doses of propofol ranging from 10 μM to 100 μM for 30 min then treated with LPS (10 ng/mL) for 24 h. Total cellular RNA was isolated and levels of IL-1β (E), TNF (F), NOS2 (G), IL-10 (H), CD206 (E), and Ym1 (F) gene expressions were determined through real time RT-PCR. Data were normalized to GAPDH and presented as fold change compared to the vehicle control group. Data are means ± SD from three experiments, each in triplicate, *, $p < .05$, **, $p < .01$ compared with the CTL group, #, $p < .05$, ##$p < .01$ compared with the LPS group.

LPS-stimulated BV2 microglial cells and used NanoSight to quantify EV concentrations. The resuspended EVs were adjusted in sterile PBS to the concentration of 5×10^{10} particles/mL and were added to the treatments groups along with LPS and propofol. The choice of this concentration of EVs is based on the levels of EV reduction caused by propofol treatment in Fig. 3. Thus, the final concentration of EVs in the treated BV2 microglial culture was 1×10^{7} particles/mL including the control. After the EV treatment, propofol-mediated downregulation of M1 marker genes (Fig. 4A-C) and upregulation of the M2 marker gene (Fig. 4D) was reversed, supporting the notion that propofol asserts anti-inflammation effects in activated microglia through the reduction of EV release.

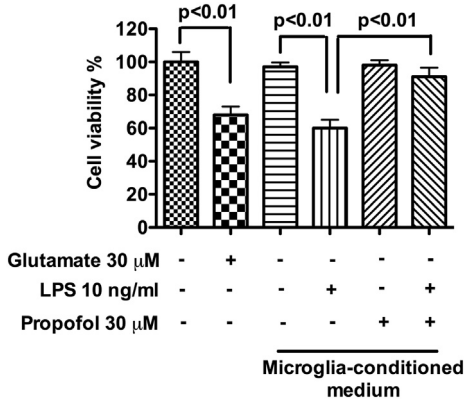

Fig. 2. Propofol inhibits microglia-mediated neurotoxicity. Microglia were pretreated with LPS for 2 h before the cultures were washed and treated with propofol at 30 μM for 24 h. Cell-free supernatants were collected from either untreated or LPS-activated microglia and added to N2A cultures for neurotoxicity. N2A cell viability was determined by the CellTiter 96® AQueous One Solution Assay at 48 h post treatment. Data are the means ± SD from three experiments.

3.5. Propofol reduces microglia-mediated neurotoxicity through reduction of EV

To investigate whether the neuroprotective effect by propofol is dependent on the reduction of EV release, we collected EVs from LPS-stimulated BV2 cells and added them to the experimental groups at the same final concentration of 1×10^7 particles/mL as in Fig. 4. In the absence of LPS, the EV treatment did not significantly alter microglia-mediated neurotoxicity toward N2A cells (Fig. 5A). In contrast, EV treatment specifically reversed propofol-mediated neuroprotection by LPS-stimulated microglia. To more specifically target MAP2-positive neurons in N2A cultures (Supplemental Fig. S3), we used a MAP2 ELSIA to quantitatively determine neuronal survival after LPS and propofol treatment. Propofol reversed neurotoxicity caused by LPS-activated microglia conditioned medium. However, such protection can be blocked by addition of EVs to microglia cultures before the collection of conditioned medium (Fig. 5B). Furthermore, LPS-activated microglia appear to induce TUNEL-positive cells in the cultures, which can be exacerbated by addition of EVs to microglia cultures before the collection of conditioned medium. Together, our data suggest that propofol pretreatment reduces activated microglia-mediated neurotoxicity by decreasing EV release.

4. Discussion

Propofol is one of the most commonly used IV drugs for the induction and maintenance of anesthesia, both during surgical procedures and during critical care sedation in intensive care units. It is used in > 50 countries and in approximately 75% of all surgeries. Here, we study the effect of propofol other than its anesthetic properties and report that in the presence of LPS, propofol is able to reduce EV release from microglia. The decrease in EV release helps rein in neuroinflammation and reduce microglia-mediated neurotoxicity. To the best of our knowledge, no study has investigated the alteration of EV release as a possible action of propofol. Our observations reveal a novel mechanism by which propofol may use to assert anti-neuroinflammation and neuroprotective effects.

Our results on the *in vitro* anti-neuroinflammation and neuroprotective effect of propofol are similar to those of Zheng et al. and Gui et al., who recently demonstrated the neuroprotective effect of propofol (Gui et al., 2012; Zheng et al., 2018). These prior studies identified miR-155, Toll-like receptor 4, and glycogen synthase kinase-3β as the key mechanisms for the neuroprotective effect of propofol. Although these mechanisms may play a significant role in anti-inflammatory responses and neuroprotection, our data showed that propofol significantly inhibits EV release from LPS-activated microglia. EVs are a heterogeneous

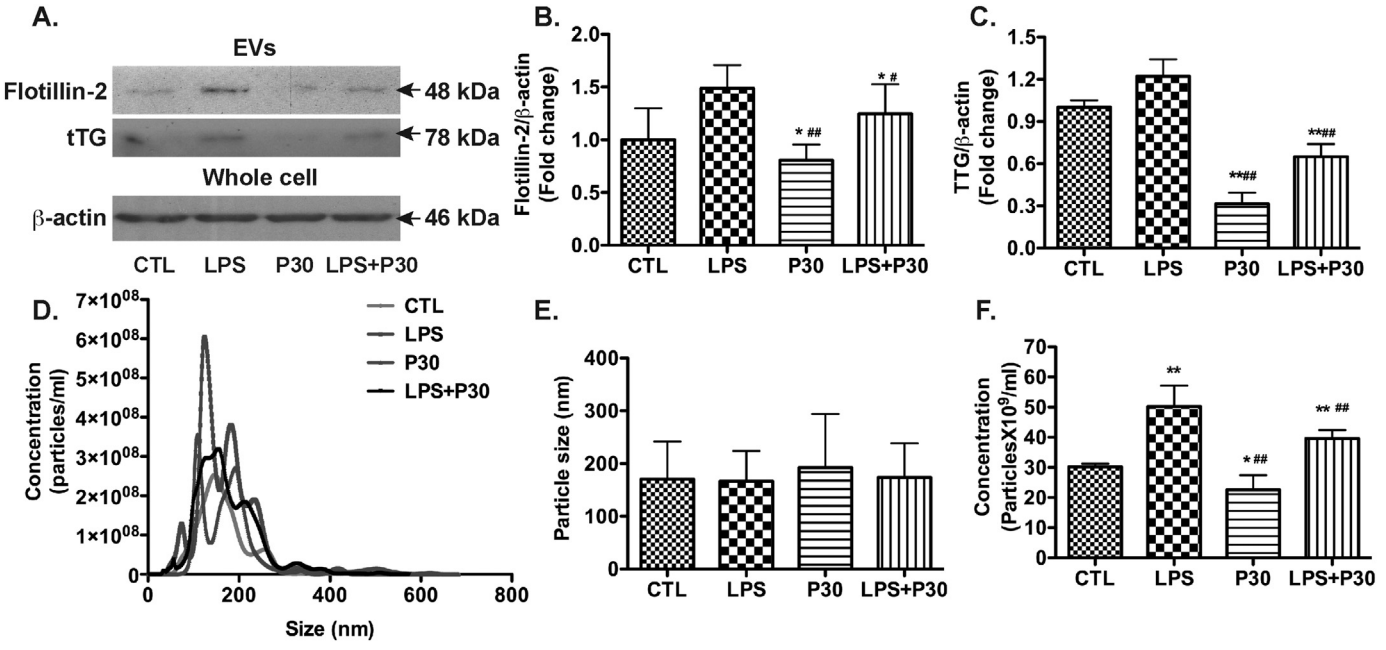

Fig. 3. Propofol inhibits EV release from LPS-stimulated microglia. BV2 microglia cells were treated with LPS (10 ng/mL) with or without propofol (30 μM) for 24 h. EVs were isolated from normalized volumes of supernatants from all experimental groups based on whole cell protein concentrations. (A-C) The levels of flotillin-2 and tTG in EVs, as well as the levels of β-actin in whole cell lysates were determined by Western blots. Densitometric quantifications of Flotillin-2 and tTG protein levels in EV markers were normalized with actin protein concentrations in whole cell lysates and presented as fold changes relative to those in vehicle control EV lysates. (D-F) EVs were visualized through NanoSight for number of EVs (1:100, y-axis) and size of EVs (nm, x-axis). Quantifications of EV number were performed through NanoSight. Results are representative of three independent experiments. Asterisk (*) and double asterisk (**) denote $p < 0.05$ and $p < 0.01$, respectively, compared to the vehicle control. The pound sign (#) and double pound sign (##) denote $p < 0.05$ and $p < 0.01$, respectively, compared to the LPS group.

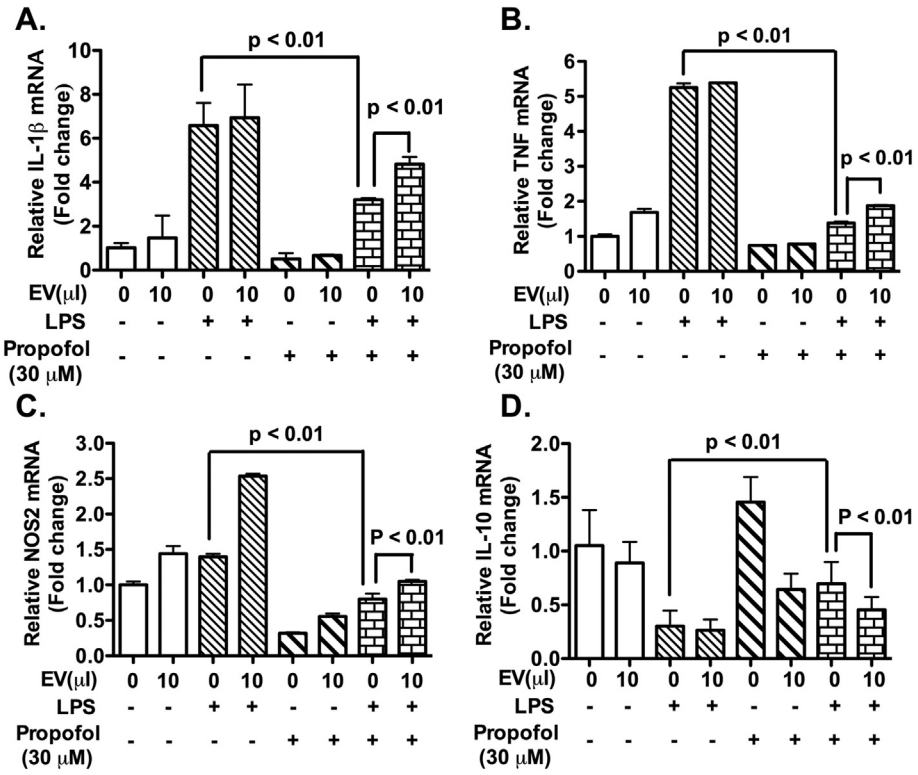

Fig. 4. Propofol blocks LPS-mediated gene expression alterations in microglia through inhibition of EV release. (A-D) BV2 microglia cells were treated with propofol (30 μM) for 30 min then with LPS (10 ng/mL) for 24 h in the presence or absence of EVs (10 ul, 5×10^8 particles) isolated from LPS-activated microglia. Total cellular RNA was isolated and levels of IL-1β (A), TNF (B), NOS2 (C), and IL-10 (D) gene expressions were determined through real time RT-PCR. Data were normalized to GAPDH and presented as fold change compared to the vehicle control group. Data are means ± SD from three experiments, each in triplicate.

group of membrane vesicles of endosomal and plasma membrane origin that are important mediators of cell-to-cell communication. EVs contain proteins, lipids, and microRNAs that can mediate various signaling functions (Mathivanan et al., 2010). EV release can be modulated by reactive oxygen species (Blanc et al., 2007), inflammation (Bianco et al., 2005), and by ATP (Savina et al., 2003). Our previous work found that immune activation induced by LPS or TNF-α can increase EV release from microglia and astrocytes, (Wang et al., 2017; Wu et al., 2015; Wu et al., 2018). In the current study, we used LPS as the inflammation-inducing agent for the microglia. Importantly, propofol markedly decreased LPS-mediated EV release in microglia, which was documented and supported by both NTA and by Western blotting analysis of EV markers. Addition of EVs can partially reverse propofol-mediated anti-neuroinflammation and neuroprotective effects in microglia, suggesting that propofol decreases microglia activation and exerts neuroprotection, at least in part, by downregulating EV release.

Because EVs are abundantly produced in the CNS and EV release is not limited to microglia, it is tempting to speculate that propofol-mediated quantitative changes of EVs may have broader implications to the CNS than neuroinflammation and neuroprotection. Indeed, the reduction in EV release by propofol is not only observed in LPS-stimulated microglia, in un-stimulated microglia in the current study, but also observed in cultured fetal human astrocytes (data not shown). Therefore, propofol-mediated downregulation of EVs might be linked to its anesthetic and extra-anesthetic properties. These possibilities are beyond the scope of this paper but strongly warrant future investigations.

In the CNS, inflammation is typically initiated by the action of microglial cells. These residential macrophages are able to respond to endogenous or exogenous stimuli and demonstrate both pathogenic and protective roles (Boche et al., 2013). Upon appropriate stimulation, classically activated, pro-inflammatory (M1) macrophages serve as one of the first lines of defense from cells of innate immunity. In many experimental models, the M1 response is characterized after exposure to bacterial-derived products such as LPS (Liu et al., 2017; Martinez and Gordon, 2014). In this study, LPS was used to activate microglia, which responded by producing M1-associated genes such as IL-1β, TNF-α, and NOS2. We found that propofol dose-dependently inhibits LPS-induced M1 gene expressions and promotes M2 gene expressions. For chronic brain injury, resident microglia become polarized toward a pro-inflammatory (M1) phenotype, which increases pro-inflammatory cytokine production, antigen presentation, and expresses high levels of inducible nitric oxide synthases for NO production (Martinez and Gordon, 2014). These microglia phenotypes are considered detrimental to the homeostasis of the brain. In contrast to M1, alternative (M2) phenotypes (Stein et al., 1992) induce expression of anti-inflammatory cytokines IL-4, IL-10, IL-13, and TGF-β, which is critical for brain repair and regeneration (Sica and Mantovani, 2012). Notably, propofol did not rescue 100% neuronal death in the initial viability assay or block IL-1β expression by LPS stimulation, raising the possibility of an EV-independent mechanism of inflammation response. This propofol effect on EVs and the potential mechanism to modulate microglia immunity may be exploited to favor tissue repair in neurological diseases.

In summary, our studies indicate that propofol can alter EVs, suggesting that this may be one aspect of its anti-neuroinflammation and neuroprotection. These new findings provide a likely mechanistic basis for the previously documented anti-neuroinflammatory and neuroprotective effects of propofol.

Conflicts of interests/financial disclosures

None.

Author contribution statement

J.L., Y.H., and J.Z. designed the research; J.L., Y.L., X.X., X.Y., R.Z. J.P., H.W., Z.T., F.G., H.L., B.W., and Y.H. performed data acquisition and analysis; J.L., Y.H., and J.Z. drafted the manuscript; all authors approved the final version of the manuscript to be published.

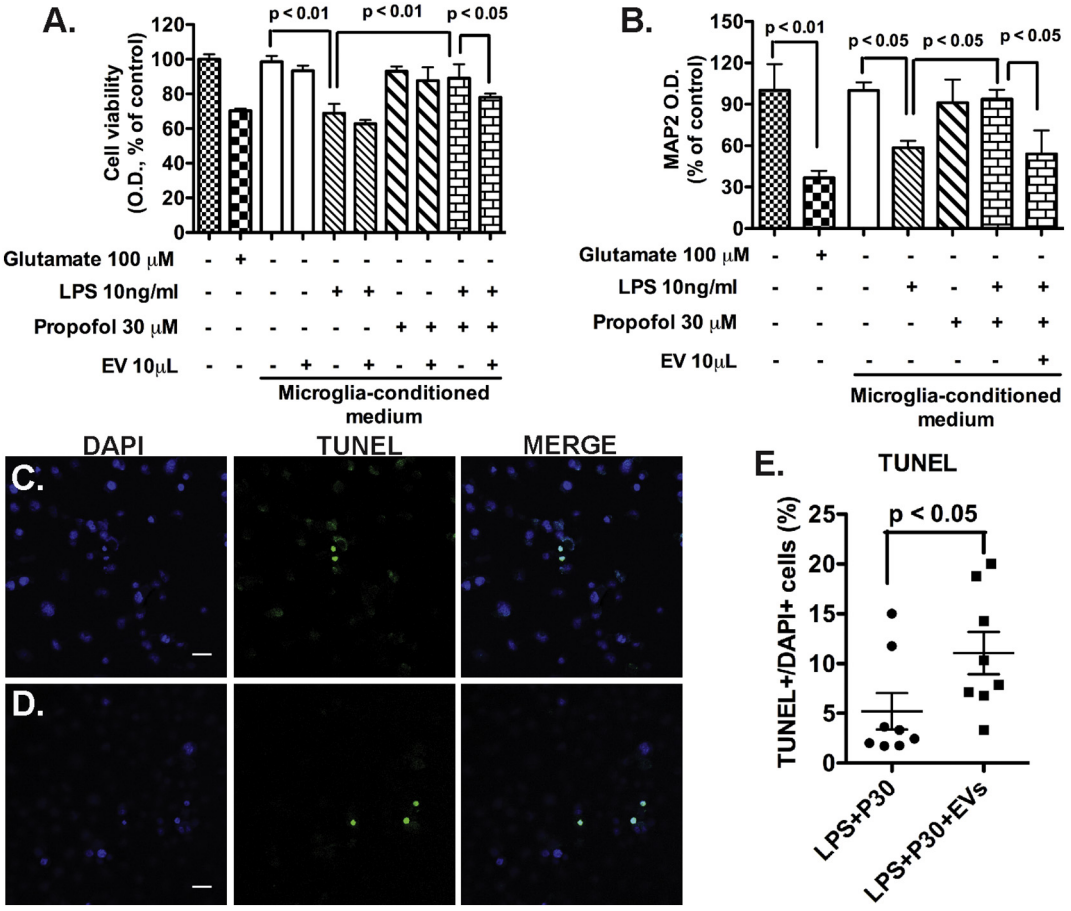

Fig. 5. Propofol reduces microglia-mediated neurotoxicity through inhibition of EV release. Microglia were pretreated with LPS for 2 h before the cultures were washed and treated with propofol at 30 μM for 24 h with or without EVs (10 ul, 5×10^8 particles) isolated from LPS-activated microglia. Cell-free supernatants were collected from microglia as conditioned medium and added to N2A cultures for neurotoxicity. (A) N2A cell viability was determined by the CellTiter 96® AQueous One Solution Assay at 48 h post treatment. (B) Neuronal loss was determined by MAP2 ELISA. (C-E) Apoptosis by conditioned medium from propofol-treated/LPS-activated microglia with (D) or without EVs (C) was determined ty the TUNEL assay. TUNEL positive cells were quantified and shown as a percentage of total cells (E). Scale bar: 20 μm. Data are the means ± SD from three experiments.

Acknowledgements

We kindly thank Dr. Zeljka Korade for providing the N2A cell line and for technical support. This work was supported by grants from National Key Basic Research Program of China (973Program Grant No. 2014CB965001 to JZ), State Key Program of the National Natural Science Foundation of China (#81830037 to JZ), Joint Research Fund for Overseas Chinese, Hong Kong and Macao Young Scientists of the National Natural Science Foundation of China (#81329002 to JZ), National Natural Science Foundation of China (#81600934 to JH), Natural Science Foundation of Shanghai, China (#16ZR1432200 to JH), and National Institutes of Health: 1R01NS097195-01 (JZ).

Appendix A. Supplementary data

Supplementary data to this article can be found online at https://doi.org/10.1016/j.jneuroim.2019.05.003.

References

Amor, S., Woodroofe, M.N., 2014. Innate and adaptive immune responses in neurodegeneration and repair. Immunology 141, 287–291.
Antonyak, M.A., Li, B., Boroughs, L.K., Johnson, J.L., Druso, J.E., Bryant, K.L., et al., 2011. Cancer cell-derived microvesicles induce transformation by transferring tissue transglutaminase and fibronectin to recipient cells. Proc. Natl. Acad. Sci. U. S. A. 108, 4852–4857.
Bianco, F., Pravettoni, E., Colombo, A., Schenk, U., Moller, T., Matteoli, M., et al., 2005. Astrocyte-derived ATP induces vesicle shedding and IL-1 beta release from microglia. J. Immunol. 174, 7268–7277.
Blanc, L., Barres, C., Bette-Bobillo, P., Vidal, M., 2007. Reticulocyte-secreted exosomes bind natural IgM antibodies: involvement of a ROS-activatable endosomal phospholipase iPLA2. Blood 110, 3407–3416.
Boche, D., Perry, V.H., Nicoll, J.A., 2013. Review: activation patterns of microglia and their identification in the human brain. Neuropathol. Appl. Neurobiol. 39, 3–18.
Choi, D.W., Maulucci-Gedde, M., Kriegstein, A.R., 1987. Glutamate neurotoxicity in cortical cell culture. J. Neurosci. 7, 357–368.
Constantino, A.A., Huang, Y., Zhang, H., Wood, C., Zheng, J.C., 2011. HIV-1 clade B and C isolates exhibit differential replication: relevance to macrophage-mediated neurotoxicity. Neurotox. Res. 20, 277–288.
Finkbeiner, S., Stevens, C.F., 1988. Applications of quantitative measurements for assessing glutamate neurotoxicity. Proc. Natl. Acad. Sci. U. S. A. 85, 4071–4074.
Fowler, C.J., 2004. Possible involvement of the endocannabinoid system in the actions of three clinically used drugs. Trends Pharmacol. Sci. 25, 59–61.
Fruhbeis, C., Frohlich, D., Kuo, W.P., Kramer-Albers, E.M., 2013. Extracellular vesicles as mediators of neuron-glia communication. Front. Cell Neurosci. 7, 182.
Gonzalez-Scarano, F., Baltuch, G., 1999. Microglia as mediators of inflammatory and degenerative diseases. Annu. Rev. Neurosci. 22, 219–240.
Gui, B., Su, M., Chen, J., Jin, L., Wan, R., Qian, Y., 2012. Neuroprotective effects of pretreatment with propofol in LPS-induced BV-2 microglia cells: role of TLR4 and GSK-3beta. Inflammation 35, 1632–1640.
Gupta, A., Pulliam, L., 2014. Exosomes as mediators of neuroinflammation. J. Neuroinflamm. 11, 68.
Huang, W.C., Lin, Y.S., Wang, C.Y., Tsai, C.C., Tseng, H.C., Chen, C.L., et al., 2009. Glycogen synthase kinase-3 negatively regulates anti-inflammatory interleukin-10 for lipopolysaccharide-induced iNOS/NO biosynthesis and RANTES production in microglial cells. Immunology 128, e275–e286.
Huang, Y., Zhao, L., Jia, B., Wu, L., Li, Y., Curthoys, N., et al., 2011. Glutaminase dysregulation in HIV-1-infected human microglia mediates neurotoxicity: relevant to HIV-1-associated neurocognitive disorders. J. Neurosci. 31, 15195–15204.
Huang, Y., Li, Y., Zhang, H., Zhao, R., Jing, R., Xu, Y., et al., 2018. Zika virus propagation and release in human fetal astrocytes can be suppressed by neutral sphingomyelinase-

2 inhibitor GW4869. Cell Discov. 4, 1–16.
Joshi, P., Turola, E., Ruiz, A., Bergami, A., Libera, D.D., Benussi, L., et al., 2014. Microglia convert aggregated amyloid-beta into neurotoxic forms through the shedding of microvesicles. Cell Death Differ. 21, 582–593.
Kochhar, G.S., Gill, A., Vargo, J.J., 2016. On the horizon: the future of procedural sedation. Gastrointest. Endosci. Clin. N. Am. 26, 577–592.
Korade, Z., Kenworthy, A.K., Mirnics, K., 2009. Molecular consequences of altered neuronal cholesterol biosynthesis. J. Neurosci. Res. 87, 866–875.
Liu, J., Gao, X.F., Ni, W., Li, J.B., 2012. Effects of propofol on P2X7 receptors and the secretion of tumor necrosis factor-alpha in cultured astrocytes. Clin. Exp. Med. 12, 31–37.
Liu, P.S., Wang, H., Li, X., Chao, T., Teav, T., Christen, S., et al., 2017. alpha-Ketoglutarate orchestrates macrophage activation through metabolic and epigenetic reprogramming. Nat. Immunol. 18, 985–994.
Martinez, F.O., Gordon, S., 2014. The M1 and M2 paradigm of macrophage activation: time for reassessment. F1000Prime Rep. 6, 13.
Mathivanan, S., Ji, H., Simpson, R.J., 2010. Exosomes: extracellular organelles important in intercellular communication. J. Proteom. 73, 1907–1920.
McGeer, P.L., McGeer, E.G., 2013. The amyloid cascade-inflammatory hypothesis of Alzheimer disease: implications for therapy. Acta Neuropathol. 126, 479–497.
Oksvold, M.P., Kullmann, A., Forfang, L., Kierulf, B., Li, M., Brech, A., et al., 2014. Expression of B-cell surface antigens in subpopulations of exosomes released from B-cell lymphoma cells. Clin. Ther. 36, 847–62 e1.
Savina, A., Furlan, M., Vidal, M., Colombo, M.I., 2003. Exosome release is regulated by a calcium-dependent mechanism in K562 cells. J. Biol. Chem. 278, 20083–20090.
Sica, A., Mantovani, A., 2012. Macrophage plasticity and polarization: in vivo veritas. J. Clin. Investig. 122, 787–795.
Smith, C., McEwan, A.I., Jhaveri, R., Wilkinson, M., Goodman, D., Smith, L.R., et al., 1994. The interaction of fentanyl on the Cp50 of propofol for loss of consciousness and skin incision. Anesthesiology 81, 820–828 (discussion 26A).
Stein, M., Keshav, S., Harris, N., Gordon, S., 1992. Interleukin 4 potently enhances murine macrophage mannose receptor activity: a marker of alternative immunologic macrophage activation. J. Exp. Med. 176, 287–292.
Stevens, B., Allen, N.J., Vazquez, L.E., Howell, G.R., Christopherson, K.S., Nouri, N., et al., 2007. The classical complement cascade mediates CNS synapse elimination. Cell 131, 1164–1178.
Suetsugu, A., Honma, K., Saji, S., Moriwaki, H., Ochiya, T., Hoffman, R.M., 2013. Imaging exosome transfer from breast cancer cells to stroma at metastatic sites in orthotopic nude-mouse models. Adv. Drug Deliv. Rev. 65, 383–390.
Thery, C., Amigorena, S., Raposo, G., Clayton, A., 2006. Isolation and characterization of exosomes from cell culture supernatants and biological fluids. Curr. Protoc. Cell Biol. 22, 1–29 Chapter 3:Unit 3.
Trapani, G., Altomare, C., Liso, G., Sanna, E., Biggio, G., 2000. Propofol in anesthesia. Mechanism of action, structure-activity relationships, and drug delivery. Curr. Med. Chem. 7, 249–271.
Vella, L.J., Greenwood, D.L., Cappai, R., Scheerlinck, J.P., Hill, A.F., 2008. Enrichment of prion protein in exosomes derived from ovine cerebral spinal fluid. Vet. Immunol. Immunopathol. 124, 385–393.
Wang, M.J., Huang, H.Y., Chen, W.F., Chang, H.F., Kuo, J.S., 2010. Glycogen synthase kinase-3beta inactivation inhibits tumor necrosis factor-alpha production in microglia by modulating nuclear factor kappaB and MLK3/JNK signaling cascades. J. Neuroinflam. 7, 99.
Wang, K., Ye, L., Lu, H., Chen, H., Zhang, Y., Huang, Y., et al., 2017. TNF-alpha promotes extracellular vesicle release in mouse astrocytes through glutaminase. J. Neuroinflam. 14, 87.
Wu, B., Huang, Y., Braun, A.L., Tong, Z., Zhao, R., Li, Y., et al., 2015. Glutaminase-containing microvesicles from HIV-1-infected macrophages and immune-activated microglia induce neurotoxicity. Mol. Neurodegener. 10, 61.
Wu, B., Liu, J., Zhao, R., Li, Y., Peer, J., Braun, A.L., et al., 2018. Glutaminase 1 regulates the release of extracellular vesicles during neuroinflammation through key metabolic intermediate alpha-ketoglutarate. J. Neuroinflam. 15, 79.
Zheng, X., Huang, H., Liu, J., Li, M., Liu, M., Luo, T., 2018. Propofol attenuates inflammatory response in LPS-activated microglia by regulating the miR-155/SOCS1 pathway. Inflammation 41, 11–19.